AIP Applied Physics Letters

Nanorod epitaxial lateral overgrowth of a -plane GaN with low dislocation density

Shih-Chun Ling, Chu-Li Chao, Jun-Rong Chen, Po-Chun Liu, Tsung-Shine Ko, Tien-Chang Lu, Hao-Chung Kuo, Shing-Chung Wang, Shun-Jen Cheng, and Jenq-Dar Tsay

Citation: Applied Physics Letters **94**, 251912 (2009); doi: 10.1063/1.3158954
View online: http://dx.doi.org/10.1063/1.3158954
View Table of Contents: http://scitation.aip.org/content/aip/journal/apl/94/25?ver=pdfcov
Published by the AIP Publishing

Articles you may be interested in

Epitaxial lateral overgrowth of a -plane GaN by metalorganic chemical vapor deposition
J. Appl. Phys. **102**, 053506 (2007); 10.1063/1.2773692

Defect reduction in (11 2 ¯ 0) a -plane GaN by two-stage epitaxial lateral overgrowth
Appl. Phys. Lett. **89**, 262105 (2006); 10.1063/1.2423328

Defect reduction in nonpolar a -plane GaN films using in situ Si N x nanomask
Appl. Phys. Lett. **89**, 041903 (2006); 10.1063/1.2234841

Improvement of microstructural and optical properties of GaN layer on sapphire by nanoscale lateral epitaxial overgrowth
Appl. Phys. Lett. **88**, 211908 (2006); 10.1063/1.2207487

Correlation of strain, wing tilt, dislocation density, and photoluminescence in epitaxial lateral overgrown GaN on SiC substrates
J. Appl. Phys. **96**, 3666 (2004); 10.1063/1.1784617

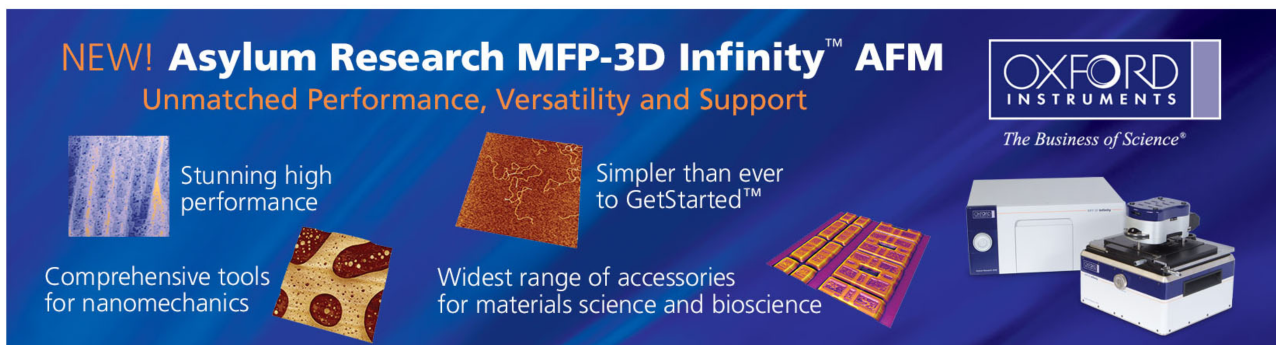

This article is copyrighted as indicated in the article. Reuse of AIP content is subject to the terms at: http://scitation.aip.org/termsconditions. Downloaded to IP: 140.113.38.11 On: Wed, 30 Apr 2014 15:01:03

Nanorod epitaxial lateral overgrowth of a-plane GaN with low dislocation density

Shih-Chun Ling,[1,a)] Chu-Li Chao,[2,3] Jun-Rong Chen,[1] Po-Chun Liu,[2] Tsung-Shine Ko,[1] Tien-Chang Lu,[1,b)] Hao-Chung Kuo,[1,b)] Shing-Chung Wang,[1] Shun-Jen Cheng,[3] and Jenq-Dar Tsay[2]

[1]*Department of Photonics and Institute of Electro-Optical Engineering, National Chiao Tung University, 1001 University Road, Hsinchu 300, Taiwan*

[2]*Electronics and Optoelectronics Research Laboratories, Industrial Technology Research Institute, 195 Chung Hsing Rd., Sec. 4 Chu Tung, Hsinchu 310, Taiwan*

[3]*Department of Electrophysics, National Chiao Tung University, 1001 University Road, Hsinchu 300, Taiwan*

(Received 20 February 2009; accepted 26 May 2009; published online 26 June 2009)

The crystal quality of *a*-plane GaN films was improved by using epitaxial lateral overgrowth on a nanorod GaN template. The investigation of x-ray diffraction showed that the strain in *a*-plane GaN grown on *r*-plane sapphire could be mitigated. The average threading dislocation density estimated by transmission electron microscopy was reduced from 3×10^{10} to 3.5×10^{8} cm^{-2}. From the temperature-dependent photoluminescence, the quantum efficiency of the *a*-plane GaN was enhanced by the nanorod epitaxial lateral overgrowth (NRELOG). These results demonstrated the opportunity of achieving *a*-plane GaN films with low dislocation density and high crystal quality via NRELOG. © *2009 American Institute of Physics*. [DOI: 10.1063/1.3158954]

Due to the existence of spontaneous and piezoelectric polarization fields, spatial separation of the electron and hole wave functions in conventional *c*-plane nitride-based quantum wells restrict the carrier recombination efficiency.[1] To avoid such polarization effects, growth along the $[11\bar{2}0]$-oriented direction has been explored for planar *a*-plane GaN on *r*-plane sapphire.[2] Recent studies of InGaN/GaN multiquantum wells demonstrate that it is possible to eliminate such polarization fields along the nonpolar orientation.[3] However, the difficulty to utilize nonpolar GaN is not a suitable substrate for heteroepitaxial *a*-plane GaN growth. In general, the threading dislocation (TD) density of $\sim3\times10^{10}$ cm^{-2} and a basal stacking fault density of $\sim3.5\times10^{5}$ cm^{-1} were commonly observed in *a*-plane GaN grown on *r*-plane sapphire.[2] The TDs in GaN act as nonradiative recombination centers which are responsible for poor internal quantum efficiency (IQE). Therefore, the reduction in TD density is essential to improve the *a*-plane device performance. Lateral epitaxial overgrowth (LEO) techniques have been employed to achieve defect reduction in nonpolar GaN. Previous LEO methods include SiN_x nanomask LEO,[4] single-step LEO,[5] selective area LEO (SALE),[6] sidewall LEO,[7] and so on. However, the regrowth thickness of these LEO techniques is usually larger than 20 μm to achieve a better coalescence surface, causing the difficulty in layer uniformity control. In this letter, we propose an approach of lateral overgrowth on nanorod *a*-plane GaN template to realize the defect reduction and quality improvement in the subsequently grown *a*-plane GaN layer. Compared with the above-mentioned LEO techniques, the nanorod epitaxial lateral overgrowth (NRELOG) is highly advantageous for thinner coalescence thickness, lower cost, and easier realization of a high-quality GaN template.

The process of NRELOG is schematically shown in Fig. 1. First, a 1.5-μm-thick *a*-plane GaN layer was grown on *r*-plane sapphire by metal-organic chemical vapor deposition (MOCVD). Then, a SiO_2 film with a 200 nm thickness and a Ni film with a 10 nm thickness were deposited in sequence to act as the etching mask. Subsequently, the thermal annealing treatment was utilized to obtain nanoscale Ni masks. The diameter of the Ni mask is 300–500 nm and the mask density is estimated to be around $6\times10^{8}/\mathrm{cm}^{2}$ as shown in Fig. 2(a). The Ni masks exhibit a random distribution with arbitrary geometries. After that, the GaN nanorods were etched through the nanomask openings by reactive ion etching (RIE)/inductively coupled plasma etching (ICP) until the height of these nanorods is 0.5 μm. The etchants for RIE were SF_6 and Ar, and the etchants for ICP etching were Ar, BCl_3, and Cl_2. Then, the SiO_2 films were deposited on the nanorods. Since the etching rate of RIE is anisotropic (the vertical etching rate is faster than horizontal etching rate), we can control the RIE parameters to remove the SiO_2 on top of *a*-plane nanorods and simultaneously leave residual SiO_2 on sidewalls of rods, as shown in Fig. 2(b). We can observe that sidewalls of GaN nanorods are passivated by a 10-nm-thick

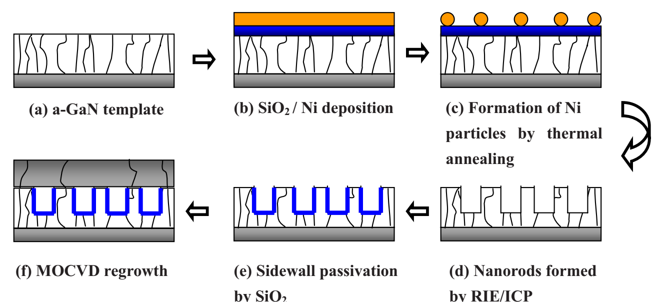

FIG. 1. (Color online) Flowchart of *a*-plane GaN NRELOG process.

a)Electronic mail: ginowell@hotmail.com.
b)Electronic addresses: timtclu@mail.nctu.edu.tw and hckuo@mail.nctu.edu.tw.

 © 2009 American Institute of Physics

This article is copyrighted as indicated in the article. Reuse of AIP content is subject to the terms at: http://scitation.aip.org/termsconditions. Downloaded to IP: 140.113.38.11 On: Wed, 30 Apr 2014 15:01:03

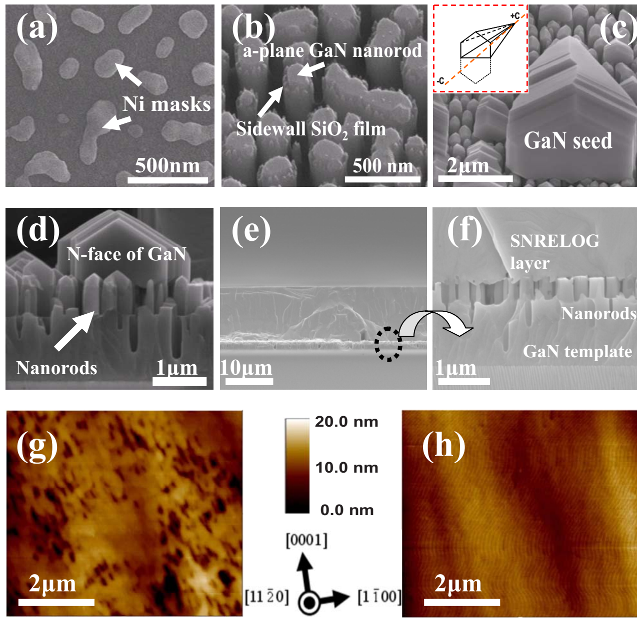

FIG. 2. (Color online) SEM images of (a) nanoscale Ni masks. (b) Fabricated GaN nanorods. (c) Initial MOCVD regrowth on *a*-plane GaN nanorods in 45° angle of view and (d) in 90° angle of view, and (e) fully coalesced *a*-plane GaN films in cross-sectional view. (f) The magnified picture of the black circular dotted line in (e). (g) and (h) 5 μm^2 AFM images of the as-grown sample and the NRELOG sample, respectively.

SiO_2 film and the top of nanorods exhibit the flat *a*-plane surface. Because the nanorods were fabricated via Ni masks, the shape and homogeneities of nanorods was similar to that of Ni masks. Finally, the GaN regrowth was performed on the nanorod template by MOCVD.

Figures 2(c) and 2(d) show the scanning electron microscopy (SEM) images of initial regrowth on *a*-plane GaN nanorods in 45° and 90° angle of view, respectively. The inset of Fig. 2(c) illustrates a GaN seed grown on the *a*-plane nanorod. Because of the sidewall passivation, the GaN regrowth along the side facets of rods was suppressed and GaN seeds only deposit on the top of nanorods. Since the growth rate in the Ga face (+*c* direction) was tenfold magnitude higher than that in N face (−*c* direction),[5] the Ga face became the arrowlike shape. The morphology of the N face became a half of hexagon and maintained mirrorlike flatness as shown in Fig. 2(d). As a result, the shape of the GaN seed was similar to that of the lying hexagonal pyramid. These GaN seeds combined with each other and finally became a fully coalesced GaN film. Figure 2(e) shows the cross-sectional SEM image of the fully coalesced GaN film. The NRELOG coalesced process can be completed within the thickness of 10 μm in comparison to the fully coalescence thickness of over 20–40 μm obtained in previous LEO techniques. Figure 2(f) exhibits the magnified picture of the black circular dotted line in Fig. 2(e). We observed that the NRELOG epilayer was suspended on the GaN nanorods due to the sidewall passivation by SiO_2. Figures 2(g) and 2(h) show the 5 μm^2 atomic force microscopy (AFM) images of the as-grown sample and the NRELOG sample, respectively. These two samples were grown under the same growth conditions (the growth temperature, pressure, and V/III ratio were 1180 °C, 200 mbar, and 800–900, respectively). Compared with the as-grown sample, the NRELOG sample apparently had the superior surface quality and less surface pits, which are believed to be originated from the TD terminations with the surface.[2] Therefore, the less surface pits show the possibility of dislocation reduction. The rms roughness of the NRELOG sample was approximately 1.9 nm, which was smaller than that of the as-grown sample (nearly 4.1 nm).

A high-resolution x-ray diffractometer (Bede D1) with a Cu target was employed to investigate the crystalline quality of GaN epilayers. All data are collected at 40 KV, 50 mA using a line focus x-ray source with 10 arc sec per step. The omega x-ray rocking curves (XRCs) on-axis $(11\bar{2}0)$ and off-axis $(1\bar{1}01)$ reflections for the as-grown (1.5/10 μm thickness) and NRELOG *a*-plane GaN samples were measured as shown in Figs. 3(a) and 3(b), respectively. It revealed that the on- and off-axis full width at half maximum (FWHM) were narrowed with increasing layer thickness due to the inclination in bulk epitaxial GaN growth. Moreover, the XRC FWHMs of the NRELOG sample on-axis and off-axis reflections were further reduced from 903 to 430 arc sec and from 1821 to 1148 arc sec with respect to the as-grown sample with 10 μm thickness. In comparison with the FWHMs of the as-grown and NRELOG samples grown to similar thickness, it is evident that the crystal quality of the *a*-plane GaN epilayer indeed could be improved with the NRELOG technique. On the basis of previous literature,[4–7] the on-axis FWHM value of NRELOG samples (430 arc sec) is even narrower than that of the SiN_x nanomask LEO (900 arc sec)/single-step ELOG sample (612 arc sec) and is comparable to that of either SALE or sidewall LEO sample (∼324 arc sec).

The typical bright-field cross-sectional transmission electron microscopy (TEM) image near $[1\bar{1}00]$ zone axis of the NRELOG sample is shown in Fig. 4(a) (acceleration voltage=120 kV). Inset presents the corresponding electron diffraction pattern. The yellow dotted lines represent the contour of GaN nanorods. Regions I and II show the nanorod template and the GaN regrowth epilayer, respectively. From

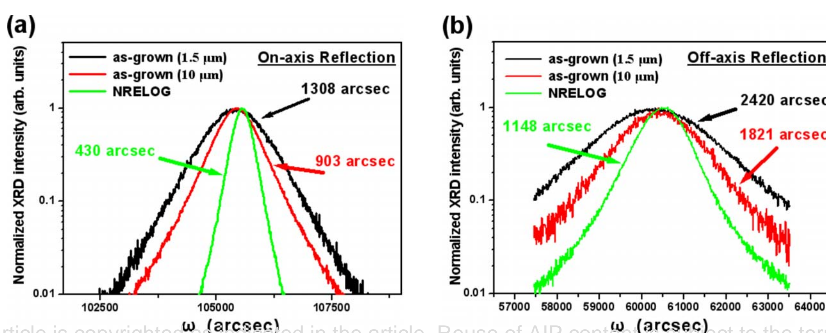

FIG. 3. (Color online) XRCs (a) on-axis $(11\bar{2}0)$ reflections and (b) off-axis $(1\bar{1}01)$ reflections for as-grown (1.5/10 μm) and NRELOG *a*-plane GaN films.

This article is copyrighted as indicated in the article. Reuse of AIP content is subject to the terms at: http://scitation.aip.org/termsconditions. Downloaded to IP: 140.113.38.11 On: Wed, 30 Apr 2014 15:01:03

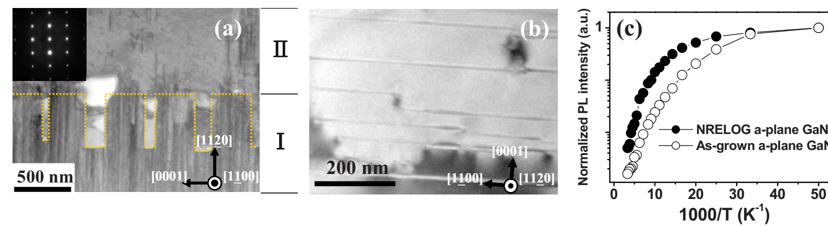

FIG. 4. (Color online) (a) Typical bright-field cross-sectional TEM image near $[1\bar{1}00]$ zone axis of the NRELOG sample. Inset shows the corresponding electron diffraction pattern. The yellow dotted lines represent the contour of GaN nanorods. (b) The plan-view TEM image near $[11\bar{2}0]$ zone axis of the NRELOG sample. (c) Arrhenius plots of the normalized integrated PL intensity over the temperature range of 20–300 K for the as-grown GaN and NRELOG GaN.

the TEM image, it is obvious that TD density in region II is much lower than that in region I. The mechanism of TD reduction by NRELOG is similar to the previous LEO methods.[4–7] The GaN seeds initially grown on the *a*-plane nanorods are the windows, and the subsequent lateral overgrown GaN are the wings. We can observe that the dislocation lines from region I penetrated into region II via the nanorods (windows). In contrast, the GaN wing between two nanorods was essentially free of dislocations. The average TD density in region II was estimated to be 3.5×10^{8} cm^{-2}, which was about two orders of magnitude lower than that in region I (3×10^{10} cm^{-2}). In addition, the stacking fault (SF) was observed from the plan-view TEM image near $[11\bar{2}0]$ zone axis as shown in Fig. 4(b). The SF density was estimated to be 2×10^{5} cm^{-1}, which was decreased by a factor of 2–3 compared to that of as-grown sample. We believe that the TD and SF density could be further decreased while the optimization of nanorod parameter is performed.

Temperature-dependent photoluminescence (PL) was utilized to investigate the quantum efficiency of the grown samples. In general, the temperature-induced quenching of luminescence involves the thermal activation of excitons to nonradiative defect states.[8] In other words, a slower intensity decline with the temperature increasing means a lower defect density in the grown sample. The normalized integrated PL intensity ratio obtained at 20 and 300 K $[I_{PL}(300\ \text{K})/I_{PL}(20\ \text{K})]$ could represent the IQE of the GaN samples. Figure 4(c) shows the normalized integrated PL intensity of GaN emission as a function of 1000/T for the as-grown sample and the NRELOG sample. The IQE obtained from $[I_{PL}(300\ \text{K})/I_{PL}(20\ \text{K})]$ value for the NRELOG GaN has a 3.4-fold increase compared to that of the as-grown GaN. The reduction in the TD density in case of NRELOG samples as compared to as-grown samples can contribute to the enhancement in the quantum efficiency and thermal activation energy.[9]

In conclusion, we have grown high-quality and fully coalesced *a*-plane GaN films by using NRELOG. The fully coalesced thickness (10 μm) of NRELOG sample was decreased by a factor of 2–4 with respect to the previous reported LEO techniques, such as ELOG, SALE, and sidewall LEO.[5–7] According to the result of TEM, the average TD density can be apparently reduced from 3×10^{10} to $\sim3\times10^{8}$ cm^{-2}. The XRC FWHMs on- and off-axis reflections were decreased from 1308 to 430 arc sec and from 2420 to 1148 arc sec, respectively, demonstrating the strain mitigation and the improvement of the crystal quality by NRELOG. Additionally, the temperature-dependent PL result showed the 3.4-fold increase in IQE compared with the as-grown GaN, which could be attributed to the TD density reduction. A series of experiments demonstrated the feasibility of using NRELOG technique to achieve the TD reduction, crystal quality improvement and the enhancement in luminescence performance in *a*-plane GaN.

This work was supported by the Ministry of Economic Affairs of the Republic of China (MOEA) and in part by the National Science Council of Taiwan under Contract Nos. NSC 96-2221-E009-094-MY3. The Grant No. of the MOEA project was 7301XS1G20 for the nonpolar GaN epitaxy and MOVPE part.

[1]T. Takeuchi, S. Sota, M. Katsuragawa, M. Komori, H. Takeuchi, H. Amano, and I. Akasaki, Jpn. J. Appl. Phys., Part 2 **36**, L382 (1997).
[2]M. D. Craven, S. H. Lim, F. Wu, J. S. Speck, and S. P. DenBaars, Appl. Phys. Lett. **81**, 469 (2002).
[3]A. Chakraborty, B. A. Haskell, S. Keller, J. S. Speck, S. P. DenBaars, S. Nakamura, and U. K. Mishra, Appl. Phys. Lett. **85**, 5143 (2004).
[4]A. Chakraborty, K. C. Kim, F. Wu, J. S. Speck, S. P. DenBaars, and U. K. Mishra, Appl. Phys. Lett. **89**, 041903 (2006).
[5]B. A. Haskell, F. Wu, M. D. Craven, S. Matsuda, P. T. Fini, T. Fujii, K. Fujito, S. P. DenBaars, J. S. Speck, and S. Nakamura, Appl. Phys. Lett. **83**, 644 (2003).
[6]C. Chen, J. Zhang, J. Yang, V. Adivarahan, S. Rai, S. Wu, H. Wang, W. Sun, M. Su, Z. Gong, E. Kuokstis, M. Gaevski, and M. A. Khan, Jpn. J. Appl. Phys., Part 2 **42**, L818 (2003).
[7]B. Imer, F. Wu, S. P. DenBaars, and J. S. Speck, Appl. Phys. Lett. **88**, 061908 (2006).
[8]Y.-h. Wu, K. Arai, and T. Yao, Phys. Rev. B **53**, R10485 (1996).
[9]J. S. Hwang, A. Gokarna, and Y,-H. Choa, J. Appl. Phys. **102**, 013508 (2007).

This article is copyrighted as indicated in the article. Reuse of AIP content is subject to the terms at: http://scitation.aip.org/termsconditions. Downloaded to IP: 140.113.38.11 On: Wed, 30 Apr 2014 15:01:03